Journal Name

COMMUNICATION

# Encapsulation of Ionic Nanoparticle Produces Reactive Oxygen Species (ROS)-Responsive Microgel Useful for Molecular Detection

Received 00th January 20xx,
Accepted 00th January 20xx

DOI: 10.1039/x0xx00000x

www.rsc.org/

Yang Liu,[a] Yu-min Wang,[c, b] Sabrina Sedano,[b] Qiaoshi Jiang,[a] Yaokai Duan,[b] Wen Shen,[b] Jianhui Jiang[c] and Wenwan Zhong*[,a, b]

**Encapsulation of ionic nanoparticles in a hydrogel microparticle, i.e. microgel, produces a target-stimulated probe for molecular detection. Selective reactive oxygen species (ROS) triggers the release of cations from the microgel which subsequently turn on the fluorogenic dyes to emit intense fluorescence, permiting rapid detection of ROS or ROS-producing molecules. The ROS-responsive microgel provides the advantages of simple fabrication, bright and stable signals, easy handling, and rapid response, carrying high promises in biomedical applications.**

Protection of functional nanomaterials with biocompatible structures like hydrogels is one feasible strategy to improve their biocompatibility and stability under physiological conditions.[1-2] The hydrophilic structures of hydrogels hold large amounts of water in their three-dimensional networks, rendering them high physiochemical similarity to the extracellular matrices.[3] Besides, enclosure of nanomaterials can improve the structural diversity and functionality of hydrogels, making it stimuli responsive.[4] Typically, responses to external stimuli, including metal ions, pH, temperature, light, added nucleic acid fuel, redox potential, etc., can be introduced via modification of the polymer structures of hydrogels.[5-8] Such stimuli-responsive hydrogels have great application potentials in controlled drug release, catalysis, programmed cell growth, and sensing.[5, 7, 9] Alternatively, encapsulation of nanoparticles (NPs) made from noble metal, metal oxide, or transition metal chalcogenides can bring in unique optical or magnetic properties to hydrogels;[10] and embedment of silica or resin NPs can increase their mechanical strength and pressure sustainability.[11]

Among all external stimuli, reactive oxygen species (ROS) are of great interest because of their imperative roles in regulating physiological processes, including signal transduction, gene expression and cell apoptosis.[12] For example, superoxide radical ($O_2^{\bullet-}$) is generated through both enzymatic and non-enzymatic oxidation process in biological systems.[13] Hypochlorite ($ClO^-$) is useful for destruction of pathogens in human body.[14] $H_2O_2$ is a stable conversion intermediate among different ROS, has the ability to cross membrane structures for signaling purposes,[15] and is involved in many enzymatic procedures as the substrate or product.[16] ROS sensors typically rely on redox enzymes that are expensive and have short shelf-life; or small chemical probes that need to be designed judiciously to possess the right redox potential and high specificity.[17] The enzyme-mimetic nanomaterials like Au,[18] CoOOH,[19] graphene oxide,[20] etc. have caught people's attention because of their high catalytic efficiency, but they require radical-based indicators with short life-time and thus produce instable signals. ROS-mediated nanoparticle decomposition to release $Ag^+$ for fluorescence quenching,[21] or to generate spectral shifts of the Ag nanoprisms,[16, 22] can be utilized for ROS detection, but the biocompatibility of such structures is questionable.

Few redox-responsive hydrogels have been reported by far, with more responding to reducing conditions via introduction of thiol groups to the polymer structures,[23-24] than to oxidation conditions, sensing of which is through enzyme encapsulation.[25-26] Herein, we report the ROS-responsive micron-sized hydrogel particles, i.e. microgel, by enclosing the ZnS-containing NPs in the gel network. The enclosed NPs are protected by the microgel from dissolution until encountering ROS, which oxidizes $S^{2-}$ and releases $Zn^{2+}$. Adding a low content of $Cu^{2+}$ to the enclosed NPs can greatly improve the microgel's responsivity to ROS owing to the formation of hydroxyl radicals (Figure 1a). Coupled with the zinc-responsive dye[27], the microgel can turn the potentially-instable presence of ROS into the stable and bright fluorescent signals, so that they can act as the sensor for ROS as well as for the ROS-producing small molecules of biomedical interest, such as glucose and cholesterol.

We prepared the microgel containing high density of carboxyl groups by emulsion polymerization of N-Isopropylacrylamide and acrylic acid using Bis-acrylamide as the crosslinker. Each gel particle

[a] *Environmental Toxicology Program, University of California, Riverside 92521, USA*
[b] *Department of Chemistry, University of California, Riverside 92521, USA*
[c] *State Key Laboratory of Chemo/Bio-Sensing and Chemometrics, College of Chemistry and Chemical Engineering, Hunan University, Changsha, Hunan, 410082, China*
† Email: Wenwan.zhong@ucr.edu

Electronic Supplementary Information (ESI) available: [details of any supplementary information available should be included here]. See DOI: 10.1039/x0xx00000x

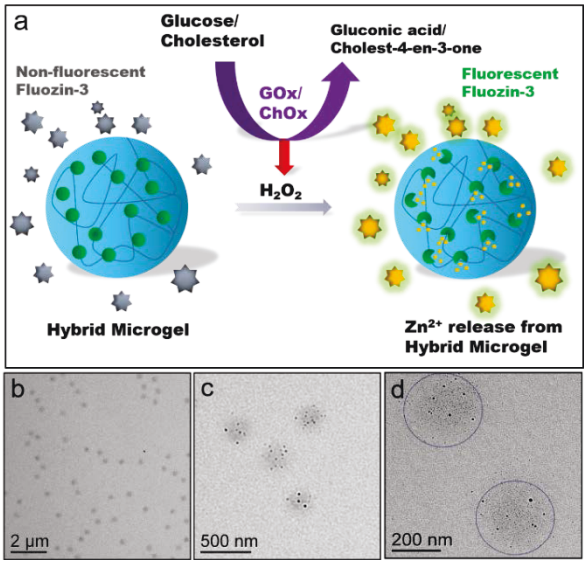


**Figure 1**. a) Scheme of microgels for detection of glucose and cholesterol. b-d) TEM images of ZnS-enclosed microgels with increasing amplification. The blue circled area in (d) is to show the enclosed nanoparticles inside the microgel.

then served as a microreactor with $Zn^{2+}$ immobilized inside the gel structure via coordination with the carboxyl groups. *In situ* synthesis of small ZnS NPs occurred with the addition of $S^{2-}$, with the polymer network helping both the nucleation and growth of the NPs, as well as limiting their sizes to less than 10 nm.[10] The size of the microgel before and after *in situ* NP synthesis were measured by the Nanosight™ with the Nanoparticle Tracking Analysis (NTA) software. Before NP encapsulation, the microgel had an average diameter around 431.1+/4.1 nm, and after NP inclusion the average size shifted slightly to 460 nm, both showing comparable size distribution (Figure S1). TEM (Figure 1b, c & d) were used to visualize clusters of small NPs locating within well separated areas (circled by arbitrary boundaries in Figure 1d), which as expected had diameters less than 5 nm. ICP-AES measurement revealed that each hydrogel particle enclosed about $1\times10^6$ $Zn^{2+}$, with the molarity of microgel estimated by NTA.

Smaller the NP is, more reactive its ions become; because the majority of the ions are displayed on the NP surface.[27-28] The high reactivity can be utilized to design stimuli-responsive structures, but the stability of the tiny NPs in biological samples is a big concern. Different from the common approaches that protect the NPs with dense surface ligands in the in-solution hydrothermal approaches,[29-30] we protected the small NPs with the hydrogel, the large amount of carboxyl groups in which could stabilize the NPs. We compared the stability of the ZnS-enclosed microgel and the 3-mercaptopropionic acid (MPA)-coated ZnS NPs (11.5 ± 2.7 nm in diameter) when stored in 1×PBS. While the microgel showed negligible release of $Zn^{2+}$ for at least one week, the MPA-coated ZnS NPs dissolved gradually and lost 50% of the Zn content within the same time period (Figure S2). Moreover, the ZnS NPs protected by hydrogel, although smaller in diameter, were more stable in acidic environment: less than 25% of the microgel-enclosed NPs dissolved after 12 hours of storage at pH 5.5, much lower than the > 60% dissolution ratio occurred to the MPA-coated NPs (Figure S3). The high stability can keep the small NP intact even in harsh environments during measurement and quickly respond to target stimulation.

On the other hand, the enclosed NPs are still accessible to small analytes that can rapidly diffuse through the gel network. Metal sulfide can be oxidized by strong oxidants like $H_2O_2$, which oxidize $S^{2-}$ to $S^0$ and then to $SO_4^{2-}$ depending on pH (Equation 1 & 2) and the redox potential of the oxidizing reagent:[31-32]

$$S^{2-} + H_2O_2 + 2\,H^+ \rightarrow S + 2\,H_2O \quad (1)$$

$$S^{2-} + 4\,H_2O_2 \rightarrow SO_4^{2-} + 4\,H_2O \quad (2)$$

Sulfide oxidation should release $Zn^{2+}$ to solutions, which can subsequently turn on the Zn-responsive dye, Fluozin-3, converting the oxidation process to fluorescent signals. For quick assessment of whether the as-prepared ZnS-enclosed microgel could be responsive to ROS and turn on the fluorescence of Fluozin-3, we treated the microgel with the representative ROS -- $H_2O_2$. Indeed, significant fluorescence increase ($F/F_0$ -1, with F being the fluorescence after reaction with ROS and $F_0$ being the initial fluorescence background from Fluozin-3) was initiated with 0.8 mM $H_2O_2$, and reached a plateau with 80 mM $H_2O_2$. Compared to the MPA-coated ZnS NPs, although the ZnS-enclosed microgel showed a relatively smaller fold of fluorescence increase at the lower [$H_2O_2$] range (0.8 – 8 mM), which also corresponded to a lower percentage of $Zn^{2+}$ released from the NP. But with a high [$H_2O_2$] of 80 mM, the microgel released $Zn^{2+}$ 2 times faster than the ZnS NP and reached a plateau fluorescence within 5 minutes (Figure 2). Using $Ag^+$ to release $Zn^{2+}$ from the microgel and turn on Fluozin-3, we confirmed that this plateau fluorescence was reached because of complete release of $Zn^{2+}$ (Figure S4). This result indicates a high [$H_2O_2$] gradient is required to deliver sufficient $H_2O_2$ into the gel to initiate $Zn^{2+}$ release from the NPs; but once the reaction is initiated, its speed is faster for the NPs enclosed in the microgel because of their smaller diameters.

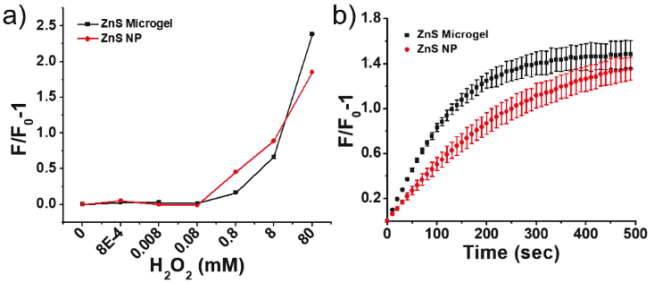


**Figure 2** a) Fluorescence response of ZnS NPs or ZnS-enclosed microgel with addition of $H_2O_2$ (incubated for 15 mins) and (b) their reaction rate with 80 mM $H_2O_2$. Total [$Zn^{2+}$] in both microgel and ZnS NP = 1.5 μM, [Fluozin-3] = 3 μM, in 1×PBS buffer at pH 7.4. $F_0$ and F represent the fluorescence before and after adding $H_2O_2$, respectively.

To enhance the responsivity to ROS, we chose to supplement $Cu^{2+}$ with $Zn^{2+}$ during cation encapsulation inside microgel, which can convert $H_2O_2$ to hydroxyl radicals (•OH) via the Fenton-like reaction,[33-34] a stronger oxidant than $H_2O_2$. Although •OH is highly reactive with organic substrates (rate constants in the range of $10^7$ $M^{-1}.s^{-1}$)[35] and cannot travel far away from where it is generated, the microgel structure keeps the $Cu^{2+}$-based •OH generation site close to the ZnS NPs, thus enhancing ZnS oxidation. Different proportions of $Cu^{2+}/Zn^{2+}$ were added during NP synthesis within the microgel, with the Cu content ranging from 1% to 50% of the Zn content in moles, keeping the total metal amount the same. The effect of $H_2O_2$-induced $Zn^{2+}$ release was evaluated using the microgel containing a

total of 1.5 μM $M^{2+}$ (confirmed with ICP-AES). We can see that, the ZnS-enclosed microgel with $Cu^{2+}$ added developed significant fluorescence increase with Fluozin-3 upon incubation with 0.08 mM $H_2O_2$, but 1% $Cu^{2+}$ showed higher fluorescence increase than the higher percentages (Figure 3a). With the supplement of 1% $Cu^{2+}$, the microgel released comparable amounts of $Zn^{2+}$ as the MPA-coated ZnS NPs at [$H_2O_2$] > 0.8 mM but detectible $Zn^{2+}$ release occurred at a [$H_2O_2$] 10 times lower (Figure S4), overcoming the diffusion problem observed above with the ZnS-enclosed microgel. The Cu-supplement also seemed to reduce the background fluorescence, generating higher fluorescence change.

We confirmed the formation of •OH mediated by $Cu^{2+}$ using chemiluminescence (CL) and electron spin resonance (ESR) spectroscopy.[36] N-(4-Aminobutyl)-N-ethylisoluminol (ABEI) can react with the oxygen-related radicals such as •OH, and produce strong CL (Figure S5a).[37-38] As shown in Figure S5a, the ZnS-enclosed microgel supplied with 1% $Cu^{2+}$ generated significantly larger CL, ~2.4 folds, compared to that without $Cu^{2+}$. Comparable CL increase was observed among the microgels prepared with 1-10% $Cu^{2+}$; but a much larger increase, ~10 folds, occurred with the addition of 50% $Cu^{2+}$. A more specific detection of •OH was carried out by ESR coupled with the radical trapping reagent of 5,5-Dimethyl-1-Pyrroline-N-Oxide (DMPO) (Figure S5b). The characteristic peaks of the typical DMPO-•OH adducts with the peak intensity ratio of 1:2:2:1 were produced with the addition of $H_2O_2$ to the ZnS-enclosed microgel supplied with 1% $Cu^{2+}$. This result supports that the supplemented $Cu^{2+}$ can greatly enhance the generation of •OH from $H_2O_2$ thus speed up $Zn^{2+}$ release from the microgel.

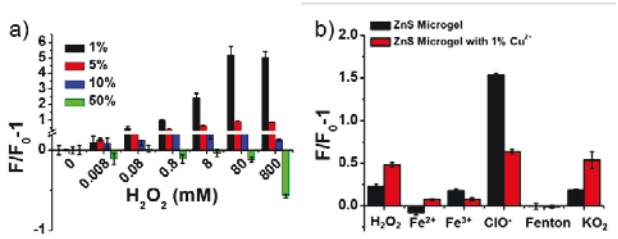


**Figure 3.** a) $H_2O_2$ measurement by ZnS-enclosed microgel with supplement of 1, 5, 10, and 50% $Cu^{2+}$ (%$Cu^{2+}$ = $Cu^{2+}$/$Zn^{2+}$×100%). b) Responsivity of the ZnS-enclosed microgel without and with the supplement of 1% $Cu^{2+}$ to various ROS. [Fluozin-3] = 3 μM, 1×PBS buffer at pH 7.4, [All reagents] = 10 μM. For Fenton reaction, 10 μM of $Fe^{2+}$ and 10 μM $H_2O_2$ was used. $KO_2$ was used to generate $O_2^{\bullet-}$.

However, supplement of $Cu^{2+}$ reduced the overall content of $Zn^{2+}$ enclosed in the microgel. Measurement of the metal composition of each microgel structure with ICP-AES after dissolving the gel with nitric acid to release all the metals (Figure S6) indicated that, with the addition of 1.5 mM pure $Zn^{2+}$, about 100 μM $Zn^{2+}$ was found in the microgel preparation, which decreased to 50 μM with the addition of 1% $Cu^{2+}$ and to < 20 μM with 5% $Cu^{2+}$, while keeping total cation concentration at 1.5 mM. When 50% $Cu^{2+}$ added, no $Zn^{2+}$ was found in the gel structure. This is because $Cu^{2+}$ binds more strongly with the carboxylic acids than $Zn^{2+}$; and the solubility constant of CuS ($K_{sp}$ = 1 x $10^{-36}$) is much lower than that of ZnS ($K_{sp}$ = 1 x $10^{-23}$), both facilitating CuS formation instead of ZnS during the nucleation and growth processes. The lower $Zn^{2+}$ content with higher %$Cu^{2+}$ greatly decreased the fluorescence signal upon NP dissolution by $H_2O_2$, making the higher %$Cu^{2+}$ structures less favorable in our sensor design.

We then tested the responsivity of the ZnS-enclosed microgel without or with the supplement of 1% $Cu^{2+}$ to various ROS (Figure 3b). All species were tested at 10 μM using the microgel containing a total [$Zn^{2+}$] = 1.5 μM. It turned out that without the addition of $Cu^{2+}$, only the strongest oxidant $ClO^-$ induced the largest fluorescence increase ($F/F_0$-1 = 1.5) from the ZnS-enclosed microgel, but no significant fluorescence increase was observed with the weaker ROS including $H_2O_2$. On the other hand, with 1% $Cu^{2+}$, $H_2O_2$, $ClO^-$ and $KO_2$ all showed comparable fluorescence increase (~ 0.5) (Figure 3b). $KO_2$ produces the unstable $O_2^{\bullet-}$ with a half-life ~0.06 s, it spontaneously scavenges and generates $H_2O_2$,[39] producing a signal comparable to that of $H_2O_2$. As discussed above, $Cu^{2+}$ can accelerate production of •OH from $H_2O_2$ that can rapidly release $Zn^{2+}$ from the microgel. Thus, copper supplement permits responses to $H_2O_2$, $ClO^-$ and $KO_2$. However, the iron species of $Fe^{2+}$ or $Fe^{3+}$ alone, and the Fenton reaction system of $Fe^{2+}$/$H_2O_2$ did not show any effects. The Fenton reaction should generate •OH, but its high reactivity does not allow it to get close to the NPs before being quenched by the polymer structure, and thus no signal was produced. Therefore, the NP-enclosed microgel we constructed should be responsive to the strong and stable ROS stimuli like $ClO^-$ and $H_2O_2$, as well as the instable ROS that can spontaneously form $H_2O_2$.

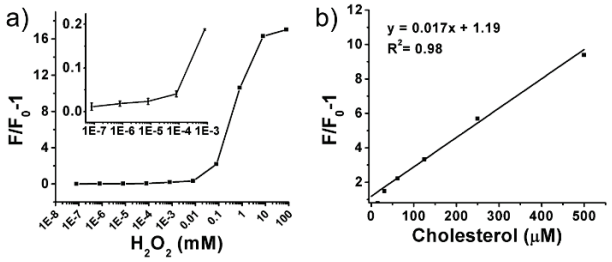


**Figure 4.** a) Calibration curve of the ZnS-enclosed microgel doped with 1% $Cu^{2+}$ for detection of $H_2O_2$. The inset enlarges the detection with the lower concentration range. b) Calibration curve for detection of cholesterol. Total [$Zn^{2+}$] in microgel = 1.5 μM, [Fluozin-3] = 3 μM, 1×PBS buffer at pH 7.4, [EDTA] = 3 μM.

The above studies support that the ROS-responsive microgel we constructed should be valuable for detection of ROS. Since some ROS like $H_2O_2$ is also involved in many enzymatic processes, the microgel can also be a versatile tool for detection of small molecular biomarkers like glucose and cholesterol. To achieve a better detection performance, we further optimized the experimental condition by reducing the fluozin-3 background using ethylenediaminetetraacetic acid (EDTA) to chelate the interfering background metals (Figure S7a&b). Under the optimized [EDTA] of 3 μM, the ZnS-enclosed microgel with 1% $Cu^{2+}$ supplement detected as low as 80 nM $H_2O_2$, and achieved a dynamic range of 80 nM to 8 mM (Figure 4a). This limit of detection is about one order of magnitude lower than most fluorescent $H_2O_2$ sensors reported previously (Table S1)[21, 40-43].

Then, we applied our microgel to detect glucose and cholesterol. The ROS-responsive microgel was added directly to the glucose-containing samples together with GOx at 2 μg/mL and reacted for 30 min (Figure S8). The presence of microgel did not affect enzyme activity in this one-pot reaction: calculation of the Michaelis–Menten constant $K_m$ using the

Lineweaver-Burke plot found a $K_m$ value of 0.54 mM, matching with previous report (Figure S10a). As low as 0.53 µM glucose was detected and a wide dynamic range up to 5 µM was achieved (Figure S9). Similarly, with 5% TX-100 added to improve target solubility (Figure S11), the LOD calculated by the 3σ method for cholesterol was found to be 0.77 µM (Figure 4b), with no impact from the microgel to the enzyme activity of ChOx (Figure S10b).[44] The simple protocol of ROS-responsive microgel to quantify glucose and cholesterol makes it a valuable tool in clinical: when applied to detect these markers in two sets of human sera, each containing 5 patient samples with various levels of glucose or cholesterol, our results agreed well with the true values provided on products information (Table S2).

To summarize, we have designed a unique ROS-responsive microgel system through NP encapsulation and cation release to turn on the fluorescence of the metal-responsive dye. Such a design carries the advantages of high structural robustness, bright and stable fluorescence signal, and easy fabrication and simple implementation. More interestingly, by tuning the NP composition, selective responsivity towards different ROS could be achieved. When applied to detect small molecular markers like glucose and cholesterol, high sensitivity, broad detection range, and accurate and fast measurement in complex biological samples can be achieved. We expect that the NP-enclosed microgels could be adopted in various biomedical applications with minor modifications in their compositions.

The authors would like to thank the support from the National Science Foundation to W.Z. via CHE-1748063.

**Conflicts of interest**

There are no conflicts to declare.

**Notes and references**


1. I. Gorelikov, L. M. Field and E. Kumacheva, *J. Am. Chem. Soc.*, 2004, **126**, 15938-15939.
2. A. Pich, A. Karak, Y. Lu, A. K. Ghosh and H. J. P. Adler, *Macromol. Rapid Commun.*, 2006, **27**, 344-350.
3. T. R. Hoare and D. S. Kohane, *Polymer*, 2008, **49**, 1993-2007.
4. M. A. C. Stuart, W. T. Huck, J. Genzer, M. Müller, C. Ober, M. Stamm, G. B. Sukhorukov, I. Szleifer, V. V. Tsukruk and M. Urban, *Nat. Mater.*, 2010, **9**, 101.
5. J. S. Kahn, Y. Hu and I. Willner, *Acc. Chem. Res.*, 2017, **50**, 680-690.
6. I. Tokarev and S. Minko, *Adv. Mater.*, 2010, **22**, 3446-3462.
7. B. Xue, V. Kozlovskaya and E. Kharlampieva, *J. Mater. Chem. B*, 2017, **5**, 9-35.
8. Y. Liu, W. Shen, Q. Li, J. Shu, L. Gao, M. Ma, W. Wang and H. Cui, *Nat. Commun.*, 2017, **8**, 1003.
9. S.-J. Jeon, A. W. Hauser and R. C. Hayward, *Acc. Chem. Res.*, 2017, **50**, 161-169.
10. J. Zhang, S. Xu and E. Kumacheva, *J. Am. Chem. Soc.*, 2004, **126**, 7908-7914.
11. W.-C. Lin, W. Fan, A. Marcellan, D. Hourdet and C. Creton, *Macromolecules*, 2010, **43**, 2554-2563.
12. K. Apel and H. Hirt, *Annu. Rev. Plant Biol.*, 2004, **55**, 373-399.
13. M. Valko, C. J. Rhodes, J. Moncol, M. Izakovic and M. Mazur, *Chem-Biol. Interact.*, 2006, **160**, 1-40.
14. D. E. Martin, J. F. A. De Almeida, M. A. Henry, Z. Z. Khaing, C. E. Schmidt, F. B. Teixeira and A. Diogenes, *J. Endod.*, 2014, **40**, 51-55.
15. B. Halliwell, *J. Neurochem.*, 2006, **97**, 1634-1658.
16. Y. Xia, J. Ye, K. Tan, J. Wang and G. Yang, *Anal. Chem.*, 2013, **85**, 6241-6247.
17. J. Xu, Y. Zhang, H. Yu, X. Gao and S. Shao, *Anal. Chem.*, 2016, **88**, 1455-1461.
18. J. Narang, N. Chauhan and C. Pundir, *Analyst*, 2011, **136**, 4460-4466.
19. Y.-M. Wang, J.-W. Liu, J.-H. Jiang and W. Zhong, *Anal. Bioanal. Chem.*, 2017, **409**, 4225-4232.
20. J. Bai and X. Jiang, *Anal. Chem.*, 2013, **85**, 8095-8101.
21. J.-L. Ma, B.-C. Yin, X. Wu and B.-C. Ye, *Anal. Chem.*, 2017, **89**, 1323-1328.
22. X. Yang, Y. Yu and Z. Gao, *ACS Nano*, 2014, **8**, 4902-4907.
23. F. Yang, J. Wang, L. Cao, R. Chen, L. Tang and C. Liu, *J. Mater. Chem. B*, 2014, **2**, 295-304.
24. S. T. K. Raja, T. Thiruselvi, A. B. Mandal and A. Gnanamani, *Sci. Rep.*, 2015, **5**, 15977.
25. K. Moriyama, K. Minamihata, R. Wakabayashi, M. Goto and N. Kamiya, *Chem. Commun.*, 2014, **50**, 5895-5898.
26. K. Moriyama, S. Naito, R. Wakabayashi, M. Goto and N. Kamiya, *Biotechnol. J.*, 2016, **11**, 1452-1460.
27. J. Yao, X. Han, S. Zeng and W. Zhong, *Anal. Chem.*, 2012, **84**, 1645-1652.
28. J. Li, T. Zhang, J. Ge, Y. Yin and W. Zhong, *Angew. Chem. Int. Ed.*, 2009, **48**, 1588-1591.
29. M. Grzelczak, J. Perez-Juste, P. Mulvaney and L. M. Liz-Marzan, *Chem. Soc. Rev.*, 2008, **37**, 1783-1791.
30. Z. Li, R. Jin, C. A. Mirkin and R. L. Letsinger, *Nucleic Acids Res.*, 2002, **30**, 1558-1562.
31. A. Chavda, M. Patel, I. Mukhopadhyay and A. Ray, *ACS Sustainable Chem. Eng.*, 2016, **4**, 2302-2308.
32. S. Aydogan, *Chem. Eng. J.*, 2006, **123**, 65-70.
33. H. Lee, H.-J. Lee, D. L. Sedlak and C. Lee, *Chemosphere*, 2013, **92**, 652-658.
34. M. B. Yim, J.-H. Kang, H.-S. Yim, H.-S. Kwak, P. B. Chock and E. R. Stadtman, *Proc. Natl. Acad. Sci. U.S.A.*, 1996, **93**, 5709-5714.
35. S. Mitroka, S. Zimmeck, D. Troya and J. M. Tanko, *J. Am. Chem. Soc.*, 2010, **132**, 2907-2913.
36. M. Liu, H. Zhang, J. Shu, X. Liu, F. Li and H. Cui, *Anal. Chem.*, 2014, **86**, 2857-2861.
37. H. Cui, Z.-F. Zhang and M.-J. Shi, *J. Phys. Chem. B*, 2005, **109**, 3099-3103.
38. Z.-F. Zhang, H. Cui, C.-Z. Lai and L.-J. Liu, *Anal. Chem.*, 2005, **77**, 3324-3329.
39. L.-Y. Zang and H. P. Misra, *J. Biol. Chem.*, 1992, **267**, 23601-23608.
40. H.-C. Chang and J.-a. A. Ho, *Anal. Chem.*, 2015, **87**, 10362-10367.
41. H. Liu, W. Na, Z. Liu, X. Chen and X. Su, *Biosens. Bioelectron.*, 2017, **92**, 229-233.
42. J. Yuan, Y. Cen, X.-J. Kong, S. Wu, C.-L. Liu, R.-Q. Yu and X. Chu, *ACS Appl. Mater. Interfaces*, 2015, **7**, 10548-10555.
43. C. Feng, F. Wang, Y. Dang, Z. Xu, H. Yu and W. Zhang, *Langmuir*, 2017, **33**, 3287-3295.
44. X. Lin, Y. Ni and S. Kokot, *Sens. Actuators, B*, 2016, **233**, 100-106.


 

Journal Name

COMMUNICATION

COMMUNICATION

Encapsulation of ionic nanoparticles in microgel produces a reactive oxygen species (ROS)-responsive probe, the encapsulated cations in which could be released by ROS to turn on fluorogenic dyes to realize detection of ROS or ROS-related biomolecules.

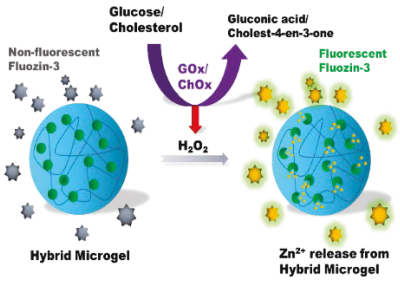


*Author(s), Corresponding Author(s)**

***Page No. – Page No.***

**Title**

# Encapsulation of Ionic Nanoparticle Produced Reactive Oxygen Species (ROS)-Responsive Microgel Useful for Molecular Detection

Yang Liu,[a] Yu-min Wang,[c, b] Sabrina Sedano,[b] Qiaoshi Jiang,[a] Yaokai Duan,[b] Wen Shen,[b] Jian-hui Jiang,[c] Wenwan Zhong *[, a, b]

[a]Environmental Toxicology Program, University of California, Riverside 92521, USA

[b]Department of Chemistry, University of California, Riverside 92521, USA

[c]State Key Laboratory of Chemo/Bio-Sensing and Chemometrics, College of Chemistry and Chemical Engineering, Hunan University, Changsha, Hunan, 410082, China

# Supporting Information

**Table of Contents:**

## 1. Experimental Section

**Materials.** N-isopropylacrylamide (NIPAM), acrylic acid (AA), bis-acrylamide (BIS), potassium persulfate (KPS), $Zn(NO_3)_2$, $Cu(NO_3)_2$, 3-mercaptopropionic acid, mercaptoacetic acid, $Na_2S$, N-(aminobutyl)-N-(ethylisoluminol) (ABEI), $H_2O_2$, NaClO, $FeCl_2$, $FeCl_3$, $KO_2$, D-glucose, cholesterol, glucose oxidase (GOx), cholesterol oxidase (ChOx) and cholesterol esterase (ChEx) were purchased from Sigma-Aldrich, Inc. (Saint Louis, MO). $Ag(NO_3)$ and Sodium dodecyl sulfate (SDS) were obtained from Fisher Scientific (Waltham, MA). Human serum samples were received from Discovery Life Sciences Inc. and stored at -80 ºC until use (Los Osos, CA). All chemicals were analytical reagent grade and used without further purification. Ultrapure water with electric resistance > 18.2 MΩ was produced by the Milipore Milli-Q water purification system (Billerica, MA).

**Synthesis of microgels.** Microgels were synthesized according to literature[1] with modifications. Briefly, 0.305 g NIPAM, 0.097 g AA, 0.03 g SDS and 4% (of total monomer) BIS were dissolved in 45 mL ultrapure water inside a three-neck flask. The solution was purged with high purity nitrogen for 30 mins at room temperature and then the temperature was increased to 70 ºC. Five milliliters of the freshly prepared KPS solution (0.002 g/mL) was added quickly to the flask and the solution was stirred for 4 hours at 70 ºC. A milk colored solution appeared after 4 hours, indicating the successful formation of the hydrogel particles. The solution was dialyzed against ultrapure water with a 12-14 kDa Spectra/Por molecular porous membrane tubing (Spectrum labs Inc., CA) to remove the non-reacted monomers and residual SDS for 2 days, replacing the dialysis solution with ultrapure water every 4 hours. The gel solution was kept at room temperature until use.

**Synthesis of ZnS or ZnSe nanoparticles.**

Briefly, for ZnS nanoparticle, 7.5 mL 0.1 M $Zn(NO3)_2$ and 0.209 mL 3-mercaptopropionic acid (MPA) were mixed and water was added to bring the volume to 42.5 mL. pH of above mixture was then adjusted to 10 with 1 M NaOH. After 30 mins of nitrogen purge, 7.5 mL 0.1 M $Na_2S$ was added and allowed to react for 20 mins. The temperature was increased to 50 ºC and kept for another 2 hours. Products were collected and cleaned by ethanol precipitation. ZnSe was prepared by heating 1.1 g Se and 7.6 g $Na_2SO_3$ in 40 mL water at 90 ºC for 2 hours with nitrogen bubbling to obtain $Na_2SeSO_3$. Then 0.35 g $ZnCl_2$ and 0.75 mL mercaptoacetic acid (MAA) were mixed in 50 mL water and pH was adjusted to 9-10 by NaOH. 5.7 mL of $Na_2SeSO_3$ solution was added.

The mixture was allowed to react at 100 ºC for 1 hour. The product was precipitated with isopropanol and dried under vacuum.

**Synthesis of ZnS- and ZnS/CuS-enclosed microgel.** The number of $COOH^-$ groups in each microgel preparation was first determined by acid-base titration. Then the microgel solution was diluted with ultrapure water to achieve a final [$COOH^-$] of ~3 mM, and $Zn(NO_3)_2$ and $Cu(NO_3)_2$ were with rapid stirring. The final molar ratio of $Zn^{2+}$: $COOH^-$ = 1:2, with varying $Cu^{2+}$ content (from 0 to 50% of $Zn^{2+}$ in moles) but the same total cation concentration of 1.5 mM. The pH was adjusted with 1 M KOH to 6.8 to ensure better coordination. After overnight incubation, the above solution was dialyzed with water for 24 hours to remove the unbounded metal ions. On the following day, $Na_2S$ was added with a final concentration of 3 mM and the reaction continued for 2 hours at room temperature. The final product was dialyzed again for 24 hours to remove the unreacted $Na_2S$ and stored at room temperature. The ZnS- or ZnS/CuS-enclosed microgels were characterized by TEM and NTA (Nanoparticles Tracking Analysis). In addition, the ZnS and ZnSe NPs coated by mercaptoacetic acid (MAA) without protection of hydrogels were also fabricated according to our previous work[2,3] and the size was determined by DLS. They were used in NP stability assessment.

**Transmission electron microscopy (TEM) and electron spin resonance (ESR).** Morphology of ZnS microgels were characterized by Transmission electron microscopy (TEM) in Philips TECNAI 12 by operating at an accelerating voltage of 22 kV. The electron spin resonance (ESR) spectra were recorded on an X-Band ESR Spectrometer (Bruker, MA, U.S.A.) following the protocol recommended by manufacturer and the Analytical Chemistry Instrumentation Facility.

**ABEI (N-(4-Aminobutyl)-N-ethylisoluminol) - $H_2O_2$ chemiluminescence detection.** One hundred μM ABEI and different microgels (ZnS and different ratios of ZnS/CuS microgel) were first mixed in 0.1 mM NaOH. The chemiluminescence signal was acquired by a Promega GloMax-Multi+ Microplate Multimode Reader with an online injection system. CL was measured immediately upon injection of $H_2O_2$. The injection rate is kept at 500 μL/s for all measurements.

**ICP-AES analysis.** Inductively Coupled Plasma - Atomic Emission Spectrometer (ICP-AES) (Norwalk, CT) was employed to verify the quantities of zinc and copper in microgels. The samples were treated with 10% $HNO_3$ before analysis. The instrument was first rinsed with 10% $HNO_3$ before injection. Standard solutions and all samples were measured in triplicate.

**Measurement of ROS.** Firstly, 10 μL of the ZnS- or ZnS/CuS-enclosed microgel was added into a well of the 96-well microplate; then, 70 μL of $H_2O_2$ and 20 μL of Fluozin-3 with or without EDTA were added to a final concentration of 3 μM. The solutions were mixed for 15 minutes on a plate shaker, before examined by a plate reader (Perkin Elmer Wallac 1420 Victor 2) with the Ex/Em wavelengths at 485/530 nm. Measurement of the responsivity to other ROS was carried out similarly, by substituting $H_2O_2$ with NaClO, $KO_2$, and Fenton reagents ($Fe^{2+}/H_2O_2$).

**Measurement of glucose and cholesterol.** Detection of glucose in solution was done as a one-pot assay, by mixing the ZnS/CuS-enclosed microgel, glucose (stock prepared in 1×PBS at 50 mM) and 2 μg/mL GOx in one well and recording the fluorescence every 3 minutes on a plate reader. Cholesterol stock solution was prepared by adding solid cholesterol into the TX-100 solution (5%, v/v) to obtain a concentration of 5 mM. A 5-minute incubation in 70 ºC water bath was necessary for complete dissolvation. Then cholesterol measurement was done in the similar way as the glucose assay, with 20 μg/mL ChOx and 0.5% TX-100 added to keep cholesterol from precipitation. For detection in serum, serum was first diluted 50 times by 1×PBS. The diluted serum was incubated with 20 μg/mL GOx (glucose detection) or 20 μg/mL ChOx/ChEx (20 μg/mL) (cholesterol detection) for 30 minutes. Then the solution was added to a 3 kDa ultra centrifugation filter (Amicon, Millipore) and centrifuged with 10,000×g for 15 minutes. The filtrate was tested by ZnS/CuS-enclosed microgel ($[Zn^{2+}]$ = 1.5 μM).

## 2. Supporting Figures

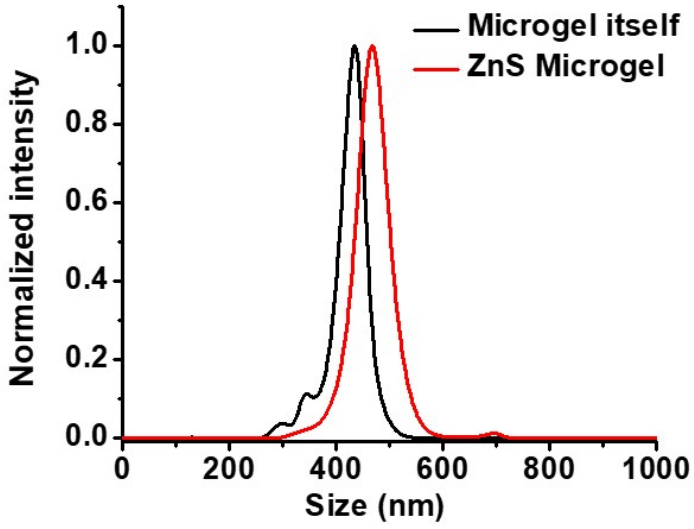


**Figure S1**. NTA measurements of size of microgel itself and ZnS-enclosed microgel.

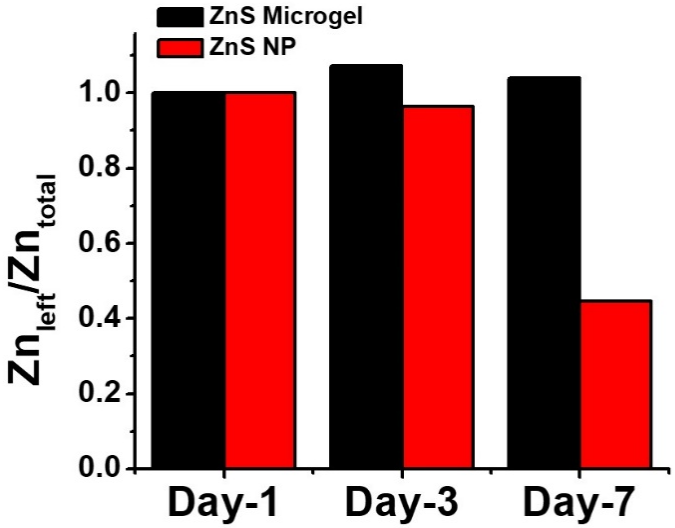


**Figure S2**. Stability of ZnS-enclosed microgel and ZnS Nanoparticle. Samples were kept in 1× PBS buffer at room temperature and measurements were made on day 1, day 3 and day 7.

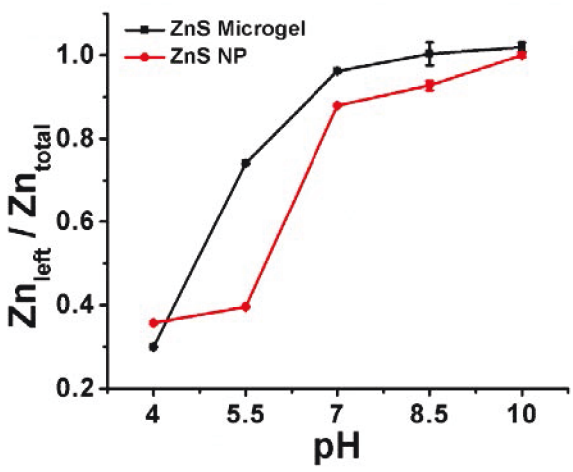


**Figure S3.** Stability of ZnS-enclosed microgel and ZnS nanoparticles in a range of pHs after 12 hours incubation.

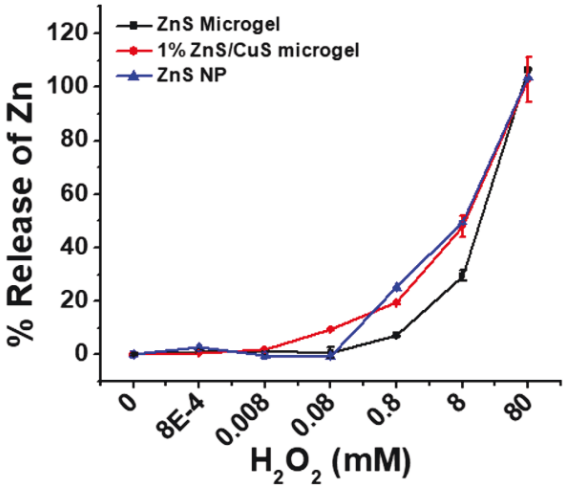


| Metal | Total | Cation exchange (100 μM $Ag^+$) | Efficiency |
|---|---|---|---|
| $Zn^{2+}$ | 27.41 μM | 26.10 μM | 95.2% |

**Figure S4.** % Release of Zn from ZnS NPs or ZnS-enclosed microgel with addition of $H_2O_2$ (incubate for 15 mins). Table: Cation exchange efficiency of ZnS microgel with addition of $AgNO_3$ and detection was done with fluorometer within 5 mins. Results obtained by ICP-AES.

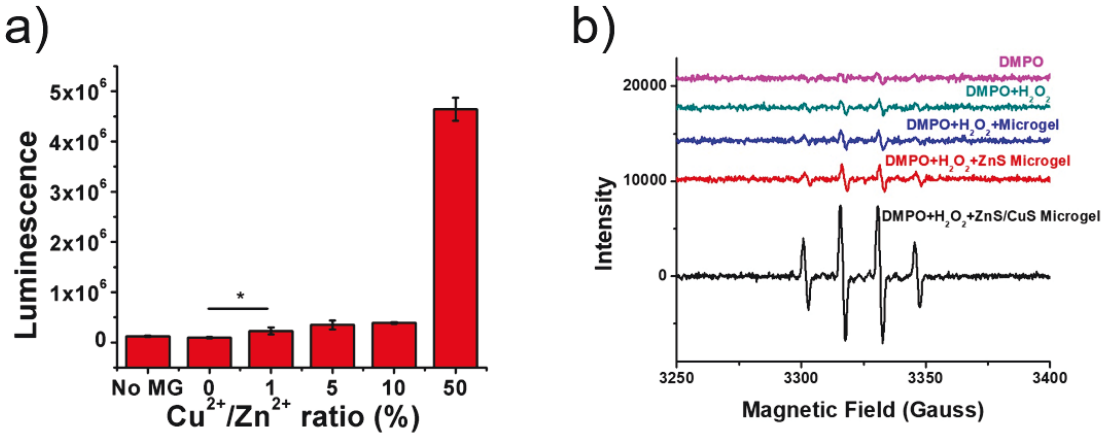


**Figure S5**. a) Chemiluminescence of different microgels with $H_2O_2$ and ABEI. [$H_2O_2$] = 1 mM, [ABEI] = 0.1 mM. b) ESR spectra of different reaction systems with DMPO as the spin trap.1% $Cu^{2+}$ was used here.

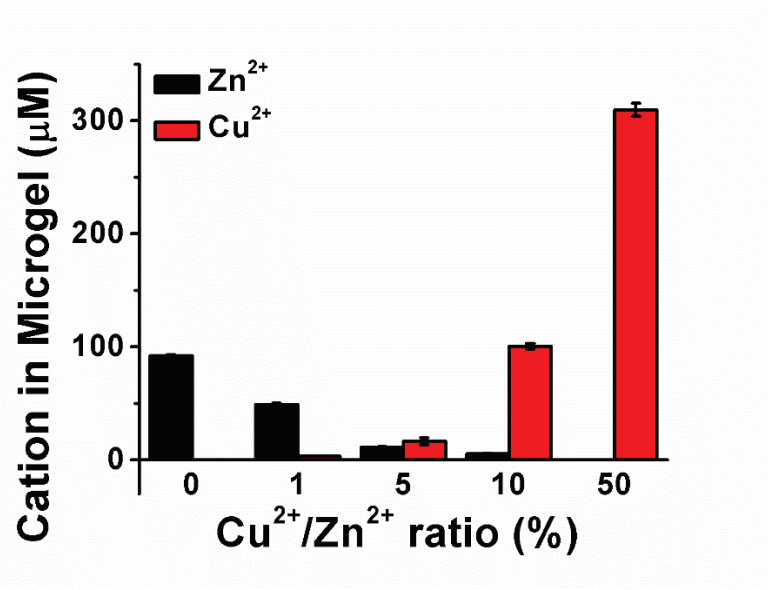


**Figure S6**. ICP-AES quantification of metal concentration in ZnS/CuS-enclosed microgel with different $Cu^{2+}/Zn^{2+}$ ratio.

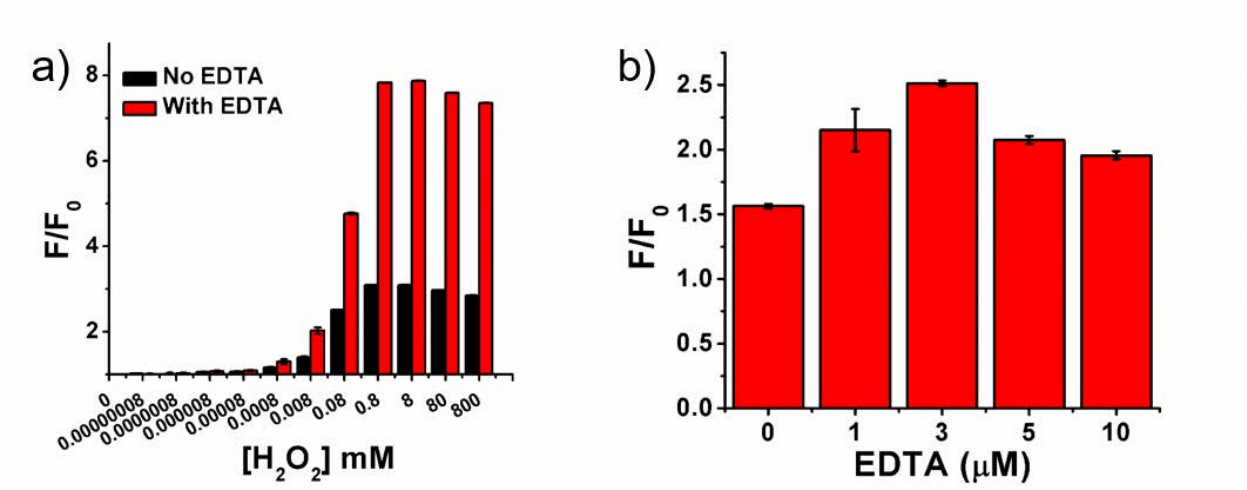


**Figure S7**. a) Fluorescence ratio change of 1% ZnS/CuS-enclosed microgel upon adding $H_2O_2$ with and without the presence of EDTA. [EDTA] = 1 μM. b) Fluorescence enhancement ratio ($F/F_0$) in response of $H_2O_2$ with different EDTA concentration. [$H_2O_2$] = 80 μM.

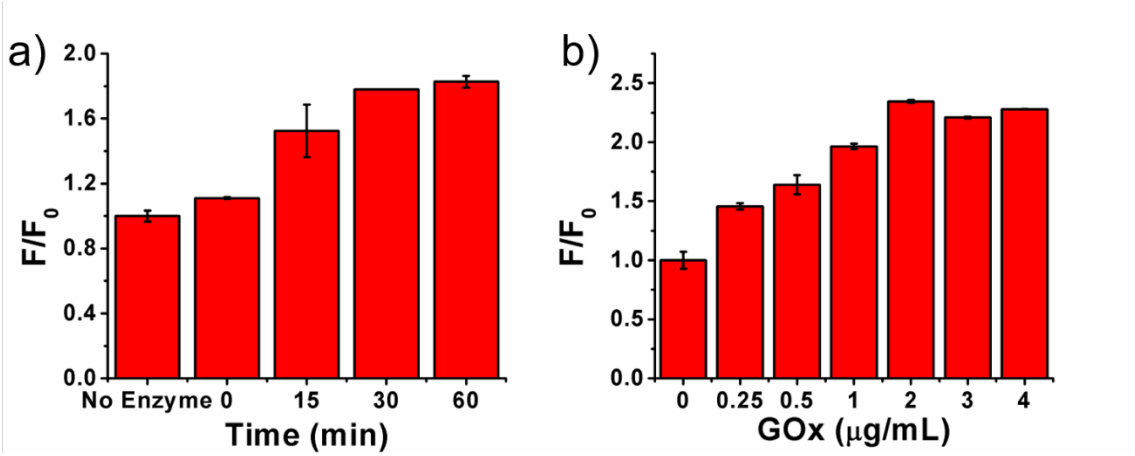


**Figure S8**. Time and enzyme concentration optimization using 100 μM glucose. a) Fluorescence ratio change of 1% ZnS/CuS-enclosed microgel with different enzyme reaction time. [GOx] = 1 μg/mL b) Fluorescence ratio change of 1% ZnS/CuS microgel with different GOx concentration, reaction time = 30 minutes.

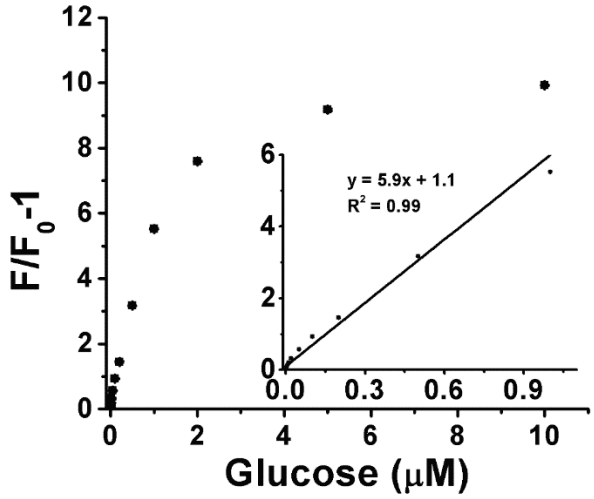


**Figure S9**. Calibration curve of glucose. Total [$Zn^{2+}$] in both microgel and ZnS NP = 1.5 μM, [Fluozin-3] = 3 μM, 1×PBS buffer, pH = 7.4. $F_0$ is the fluorescence before adding $H_2O_2$, F is the fluorescence after adding $H_2O_2$.

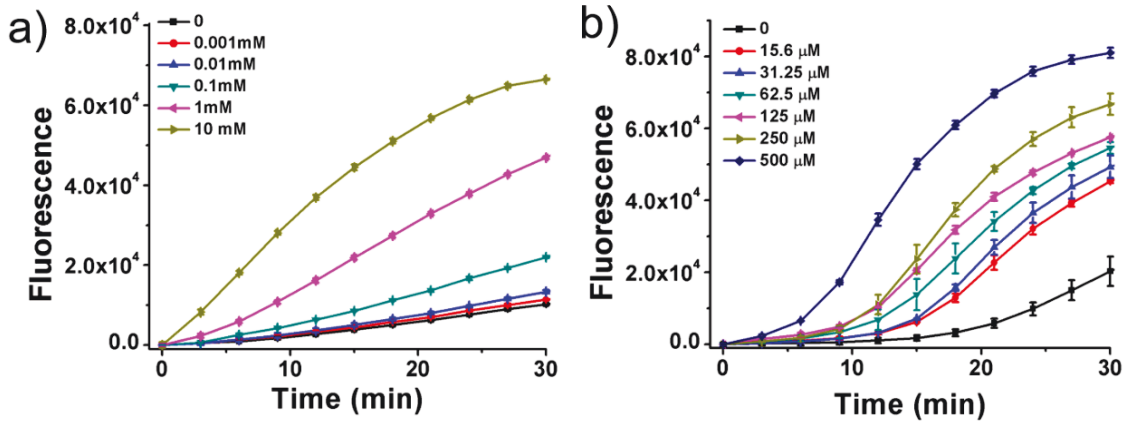


**Figure S10.** Continuous monitoring of GOx activity with different concentrations of (a) glucose, from 0 to 10 mM and (b) cholesterol, from 0 to 500 μM.

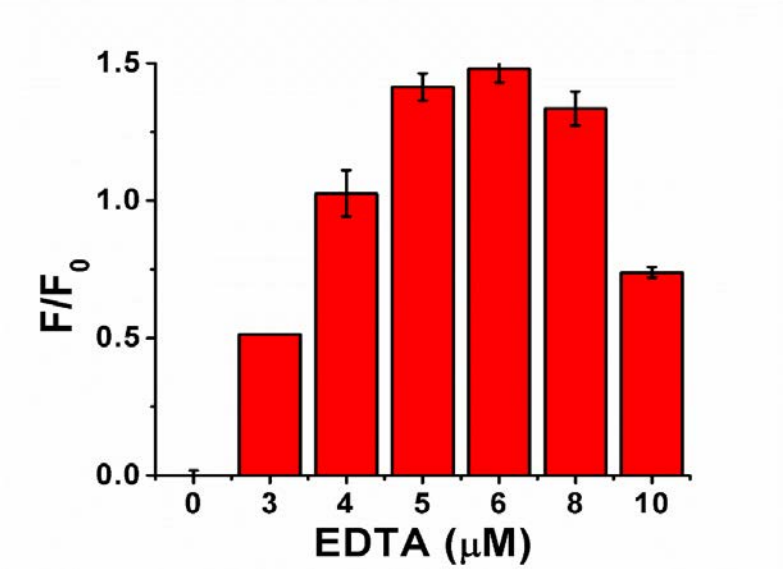


**Figure S11**. EDTA optimization for cholesterol detection. 5% TX-100 was used to dissolve the cholesterol.

## 3. Supporting Tables

**Table S1.** Comparison of our method to other methods using fluorescence as signal output.

| Methods | Dynamic Range (μM) | LOD (μM) | Reference |
|---|---|---|---|
| GelRed/$[G_3T]_5/Tb^{3+}$ | 0-100 | 3.6 | 4 |
| graphene quantum dots | 1.11-300 | 0.32 | 5 |
| Carbon dots | 0-400 | 0.01 | 6 |
| Graphitic carbon nitride | 0-2,000 | 0.05 | 7 |
| Fluorescent probe | 0-30 | 2.1 | 8 |
| $MnO_2$ nanosheet | 0-150 | 0.9 | 9 |
| Polymeric nanoprobe | 0-500 | 0.76 | 10 |
| Carbon dots/AgNPs | 2-100 | 1.39 | 11 |
| Gold Nanocluster | 1-100 | 0.8 | 12 |
| ZnS/CuS Microgel | 0-8,000 | 0.08 | Our work |

**Table S2.** Real serum sample tests. Cholesterol esterase was added to hydrolyze cholesterol ester in serum and produce cholesterol before measurement with the microgel and ChOx.

| Sample | Product Info. (Glucose mM) | This method (Glucose mM) | RSD |
|---|---|---|---|
| 1 | 5.83 | 6.93 | 4.44% |
| 2 | 25.4 | 25.86 | 1.79% |
| 3 | 2.94 | 3.74 | 6.53% |
| 4 | 16.11 | 17.61 | 4.07% |
| 5 | 10.39 | 11.44 | 6.57% |
| Sample | Product Info. (Cholesterol mM) | This method (Cholesterol mM) | RSD |
| 6 | 1.94 | 2.03 | 1.79% |
| 7 | 3.37 | 3.87 | 1.08% |
| 8 | 6.14 | 5.45 | 8.55% |
| 9 | 10.98 | 11.08 | 1.08% |
| 10 | 8.8 | 8.13 | 6.92% |

## 4. References


1. J. Zhang, S. Xu and E. Kumacheva, *J. Am. Chem. Soc.*, 2004, **126**, 7908-7914.

2. J. Yao, X. Han, S. Zeng and W. Zhong, *Anal. Chem.*, 2012, 84, 1645-1652.

3. J. Yao, S. Schachermeyer, Y. Yin and W. Zhong, *Anal. Chem.*, 2011, 83, 402-408.

4. J.-Q. Chen, S.-F. Xue, Z.-H. Chen, S. Zhang, G. Shi and M. Zhang, *Biosens. Bioelectron.*, 2018, **100**, 526-532.

5. H. Liu, W. Na, Z. Liu, X. Chen and X. Su, *Biosens. Bioelectron.*, 2017, **92**, 229-233.

6. Y. Ma, Y. Cen, M. Sohail, G. Xu, F. Wei, M. Shi, X. Xu, Y. Song, Y. Ma and Q. Hu, *ACS Appl. Mater. Interfaces*, 2017, **9**, 33011-33019.

7. J.-W. Liu, Y. Luo, Y.-M. Wang, L.-Y. Duan, J.-H. Jiang and R.-Q. Yu, *ACS Appl. Mater. Interfaces*, 2016, **8**, 33439-33445.

8. M. Ren, B. Deng, K. Zhou, X. Kong, J.-Y. Wang and W. Lin, *Anal. Chem.*, 2017, **89**, 552-555.

9. J. Yuan, Y. Cen, X.-J. Kong, S. Wu, C.-L. Liu, R.-Q. Yu and X. Chu, *ACS Appl. Mater. Interfaces*, 2015, **7**, 10548-10555.

10. C. Feng, F. Wang, Y. Dang, Z. Xu, H. Yu and W. Zhang, *Langmuir*, 2017, **33**, 3287-3295.

11. J.-L. Ma, B.-C. Yin, X. Wu and B.-C. Ye, *Anal. Chem.*, 2017, **89**, 1323-1328.

12. H.-C. Chang and J.-a. A. Ho, *Anal. Chem.*, 2015, **87**, 10362-10367.